Investigation of Free Base, Mg, Sn, and Zn Substituted Porphyrin LB Films as Gas Sensors for Organic Analytes

Alan D. F. Dunbar,[†],* Tim H. Richardson,[†] Alex J. McNaughton,[†] Jordan Hutchinson,[‡] and Chris A. Hunter[‡]

Department of Physics and Astronomy, University of Sheffield, Hicks Building, Hounsfield Road, Sheffield S3 7RH, U.K., and Department of Chemistry, University of Sheffield, Dainton Building, Brook Hill, Sheffield, S3 7HF, U.K.

Received: April 28, 2006; In Final Form: June 29, 2006

The visible absorption spectra of various substituted porphyrin compounds both in chloroform solution and as Langmuir−Blodgett (LB) solid-state films have been investigated. The porphyrin compounds examined were the Zn, Sn, Mg, and free base derivatives of 5,10,15,20-tetrakis[3,4-bis(2-ethylhexyloxy)phenyl]-21*H*,-23*H*-porphine (EHO). Changes in the absorption spectra of these materials induced by their exposure to various organic compounds are reported with a view toward determining whether this is a useful approach toward an optical gas sensor.

Introduction

Concerns about toxins released either maliciously or inadvertently by combustion engines and various industries have continued to increase. Therefore, the need for accurate and reliable sensors to detect a broad spectrum of organic compounds has never been greater than it is now. Accurate information about the impact of these toxins upon the environment, and the health and safety of those living and working close to their sources, cannot be collected until affordable, accurate, and reliable sensors to quantify the presence of such toxins have been developed. Such concerns have led to more stringent legislation regarding the production of toxins;[1,2] however, for such legislation to make a difference, it is necessary to be able to accurately monitor the levels of such gases being produced at a minimum cost. Therefore, there is increasing motivation to develop more economical gas sensors capable of monitoring low concentrations of toxic gases.

At present, the readily available gas sensors include those that use semiconducting metal oxides such as tin, tungsten, or chromium titanium oxides.[3,4] These materials change conductivity when they interact with an oxidizing (e.g., NO_2) or reducing (e.g., H_2) analyte. The conductivity change is measured, and therefore, the presence of the oxidizing or reducing gas is determined. These devices do not respond well to humid conditions, and they require high operating temperatures, ∼150−600 °C. Other well-known sensor devices include liquid electrolyte fuel cells and infrared sensors.[5] Conducting polymers[6] have achieved limited success as "electronic nose" devices, and phthalocyanines have attracted attention as semiconductometric sensors.[7] However, the majority of these organic sensors suffer from slow response times and incomplete recovery in the absence of the analyte gas.

Porphyrins possess distinctive UV−vis absorption spectra due to their highly conjugated π-electron systems.[8] If the analyte under investigation has a sufficiently strong interaction with the porphyrin, the energies of the conjugated π-electrons in the porphyrin are shifted, and hence, the absorption spectra change. Considerable work has already been performed to develop a porphyrin-based sensor system for NO_2.[9−12] Some of the porphyrin-based sensors can be recovered by gentle heating (∼90 °C) and are therefore reuseable.[10] The concentration dependence of porphyrin thin films has been found to follow a Langmuir adsorption model at low concentrations (0.46−4.6 ppm).[12] Porphyrin sensors are also being incorporated into single use colorimetric sensor arrays to detect volatile organic compounds.[13]

This work is a study of four different porphyrins, EHO in its free base form and also metalated with Sn, Mg, and Zn. We compare the reaction of these porphyrins with a range of different volatile organic compounds; the aim of this work is to determine the suitability of the four porphyrins studied for use as optical-based gas sensors for the different volatile organic analytes. First, each of the four porphyrins was tested in solution for changes in the optical absorption upon exposure to the full range of analytes. The results of this preliminary study were then used to guide the choice of porphyrins to be selected for fabrication of solid-state LB films, which were subsequently tested for sensor action with the corresponding analytes. The materials and experimental procedures used are described in the next section followed by discussion of the results for the solution experiments. This is followed by discussion of the results for the solid-state LB films, and finally, some conclusions are made.

Experimental Section

Materials. The synthesis of 5,10,15,20-tetrakis[3,4-bis(2-ethylhexyloxy)phenyl]-21*H*,23*H*-porphine has been described elsewhere,[10] and its chemical structure is shown in Figure 1a. Upon metalation, the two hydrogen atoms in the center of the porphyrin ring are replaced with the corresponding metal ion. The metal derivatives of 5,10,15,20-tetrakis[3,4-bis(2-ethylhexyloxy)phenyl]-21*H*,23*H*-porphine were prepared in accordance with literature methods.[14] Zinc was inserted into the

---

* To whom correspondence should be addressed. Phone: +44 114 222 4543. Fax: +44 114 272 8079. E-mail: a.dunbar@shef.ac.uk.

[†] Department of Physics and Astronomy.

[‡] Department of Chemistry.

10.1021/jp0626059 CCC: $33.50

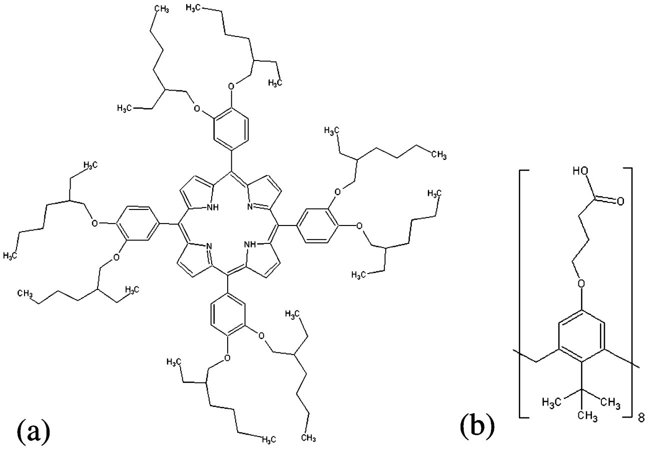

Figure 1. Chemical structure of (a) 5,10,15,20-tetrakis[3,4-bis(2-ethylhexyloxy)phenyl]-21*H*,23*H*-porphine and (b) carboxylic acid substituted calix[8]arene.

porphyrin by using excess zinc acetate in dichloromethane at room temperature. Similarly, at room temperature and in dichloromethane, the magnesium porphyrin was prepared using magnesium bromide ethyl etherate and triethylamine. To insert tin, the free base porphyrin was refluxed with tin(II) chloride in pyridine and was then stirred with sodium hydroxide solution. All three metalloporphyrins upon reaction completion were purified using grade IV aluminum oxide column chromatography. Synthesis of the carboxylic acid substituted calix[8]arene is described elsewhere,[15] and its structure is shown in Figure 1b. The analytes used are 1-octanol, hexylamine, octanal, acetic acid, 1-hexanethiol, 2-butanone, ethyl acetate, trimethyl phosphite, octylamine, and triethylamine. They were all provided by Sigma Aldrich and used as supplied.

Experimental Methods. Solutions of the free base and metalated EHO were prepared at concentrations of 4.0×10^{-6}, 3.2×10^{-6}, 2.6×10^{-6}, and 4.0×10^{-6} M of the free base, Mg, Sn, and Zn EHO, respectively, using chloroform as the solvent. These EHO solutions (2 mL portions) were placed in quartz cuvettes, and initial absorption spectra of the solutions were recorded using an Ocean Optics USB2000 spectrometer with a Mikropack Mini D2 UV−vis−IR light source. The absorbance spectra for each were calculated in the range 350−850 nm with respect to a reference taken of chloroform. The analyte to be investigated was then added 20 μL at a time, and the mixture was then stirred. Analyte was added until no further spectral changes were noticed, and then, the exposed spectrum was recorded. This process was repeated for the four EHOs with each of the 10 different analytes described in the Materials subsection.

Absorbance spectra of each of the analytes on their own were also recorded, with respect to an empty quartz cuvette reference, to confirm the range of optical transparency of each analyte.

Langmuir−Blodgett films of each of the EHOs were prepared from the chloroform solutions. For the initial experiments, solutions of just the EHO were used. However, for later experiments the EHO solutions were mixed with a solution of calix[8]arene in an EHO/calix[8]arene 1/2 molar ratio. A 150 μL portion of the EHO or EHO/calixarene solution (∼0.3 mg/mL) was spread on a clean water (Elga PURELab Option >15 MΩcm) subphase surface in a NIMA model 611 Langmuir Blodgett trough. After evaporation of the solvent, the film was compressed to and then held at a surface pressure of 40 mN/m while deposition onto a glass plate (rendered hydrophobic by exposure to 1,1,1,3,3,3-hexamethyldisilazane vapors for 12 h) was carried out. Deposition was performed by dipping the glass plate vertically at a rate of 10 mm/min. There were 10 excursions performed for each plate, resulting in the deposition of 20 layers (one layer for each of the up and down strokes). If necessary, so as to maintain the surface pressure at 40 mN/m the deposition was halted while the trough barrier was retracted and an additional 125 μL of the mixed solution was added to the subphase before recompressing to 40 mN/m again and continuing the deposition.

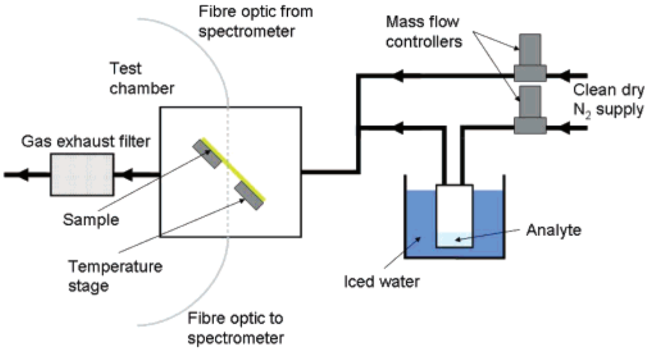

Figure 2. Schematic diagram of the gas sensor testing apparatus.

A purpose built sensor testing chamber was used to expose the solid-state sensor films to the analyte vapors, see Figure 2. The delivery of clean dry nitrogen to a chamber containing the analyte was controlled with a Tylan FC-260 mass flow controller. The temperature of the analyte was maintained at 0 °C by submerging the analyte chamber in iced water, therefore mixing the N_2 gas with the analyte at a known vapor pressure. This cooling of the gas also helped to reduce contamination problems due to condensation of the analytes onto the walls of the delivery pipes which were at room temperature and therefore warmer then the analyte vapors. The resultant mixture was then further mixed with a second supply of N_2 controlled with a second Tylan FC-260 mass flow controller and then fed into the test chamber. The solid-state film to be tested was mounted in the test chamber on a Peltier heating stage capable of controlling the film temperature in the range 5−52 °C. The temperature stage has a hole through the center such that there is a clear optical path between the two optical fibers used to deliver and collect the light for the optical measurements. The fibers were connected to a World Precision Instruments Spectromate spectrophotometer which incorporates a tungsten white light source and a multichannel photodiode detector allowing the absorption spectra of the film under test to be recorded in situ every 3 s over the spectral range 350−850 nm. The exhaust gas passes through an activated charcoal filter to absorb the toxic vapor before being vented to the atmosphere. The presence of analyte vapors in the test chamber was found to cause increased scattering and therefore increase the optical absorbance at all wavelengths. In these experiments, such effects were accounted for by subtracting a reference absorbance (measured at 800 nm where all the samples investigated are transparent) from the recorded experimental data.

Results and Discussion

The initial absorption spectra for the four different EHO solutions are shown in Figure 3. For the free base EHO, the distinctive Soret absorption band at 426 nm is much more intense than the four weak Q-bands at 519, 556, 592, and 650 nm. For the Mg EHO, the Soret band occurs at 430 nm with only two weak Q-bands at 565 and 610 nm. There are only two Q-bands at longer wavelengths for Mg EHO and the other

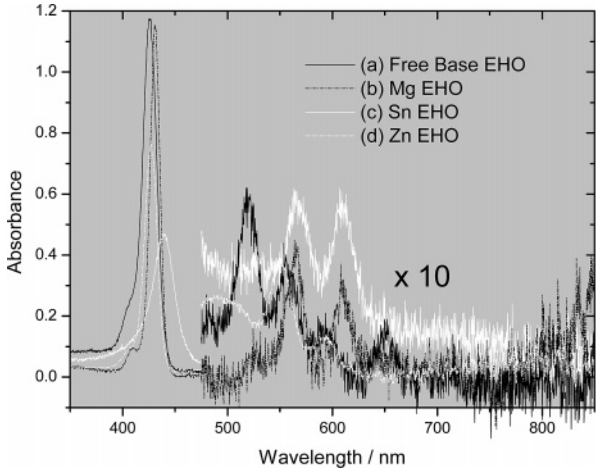

Figure 3. Absorbance spectra for (a) free base (solid black), (b) Mg (dashed black), (c) Sn (solid white), and (c) Zn EHO (dashed white) solutions in $CHCl_3$ (the spectra from 475 to 850 nm have been multiplied by 10).

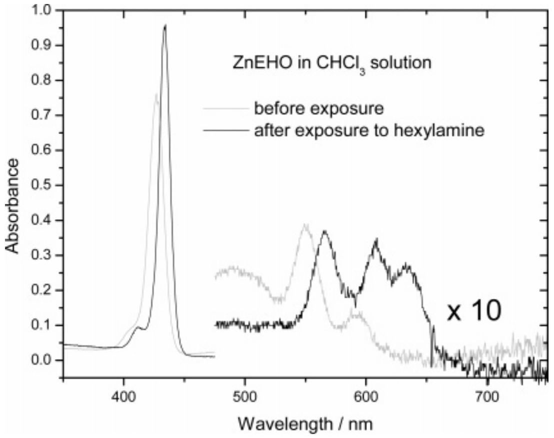

Figure 4. Absorbance spectra for a solution of ZnEHO before (gray) and after (black) exposure to hexylamine (the spectra from 475 to 750 nm have been multiplied by 10).

metalated EHOs because they have increased symmetry, therefore making the energy levels involved in the Q-band absorption degenerate and thus reducing the number of visible absorption bands from four to two. The Sn EHO solution has its Soret absorption at 440 nm with Q-bands at 564 and 608 nm, and finally, the Zn EHO solution has its Soret absorption peak at 427 nm with Q-bands at 550 and 592 nm.

The absorption spectra of the different analytes were measured, and it was found that all the analytes are highly transparent from 350 to >850 nm. Short wavelength (<350 nm) absorption features which were observed in some of the interaction experiments (data not shown) containing octanal, butanone, and triethylamine are simply due to absorption by unreacted analyte in the solution rather than due to any interaction with the EHO.

The spectra for Zn EHO before and after exposure to hexylamine are shown in Figure 4 as an example of a strongly interacting EHO/analyte pair. To be useful as an optical sensor, the absorption spectrum of the sensor material must change upon exposure, as is the case in Figure 4. Zinc(II) porphyrins are well-known to coordinate nitrogen ligands to form 5-coordinate complexes[16] with an associated change in the Soret absorption spectrum because the metal is pulled slightly out of the plane of the porphyrin in the complex that is formed. The trend for ZnEHO exposure to amines is for the Soret absorbance band to both shift slightly to longer wavelength (from 427 to 433 nm for hexylamine) and also increase in intensity (by ~24% for hexylamine). Meanwhile, the two Q-bands shift to longer wavelengths, and often more than two Q-bands appear. The magnitude of the Soret band shift and the intensity change appear to be dependent upon the amine used during the exposure. This effect is the focus of further investigations.

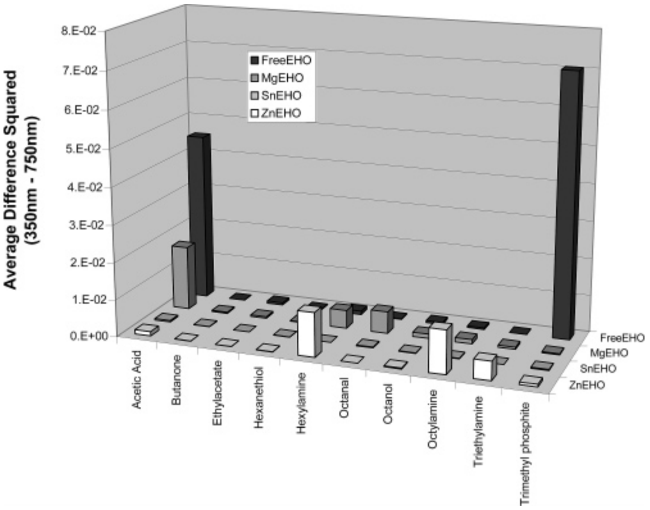

Figure 5. Average of the square of the difference between the before exposure spectrum and the after exposure spectrum for the free base, Mg, Sn, and Zn EHOs and 10 different analytes.

For the free base EHO, which has a strong interaction with acetic acid and trimethyl phosphite, the Soret peak is replaced by a broader, lower intensity peak at longer wavelength (~465 nm), and the four Q-bands initially present are replaced with a single broader but more intense absorbance band at much longer wavelength (~700 nm), as is also the case for free base EHO upon exposure to NO_2.[17]

It was noted that, upon exposure of MgEHO to acetic acid, there was a slow interaction during which the absorbance spectrum changed from that which is characteristic of MgEHO to that which is typical for the free base EHO before then partially undergoing a further change similar to that observed when free base EHO is exposed to acetic acid. It has been well documented that Mg(II) porphyrins are demetalated by acids to form the corresponding free base porphyrin.[18] It is therefore likely that exposure to acetic acid causes the conversion of MgEHO back to the free base EHO. There are also weak responses noted for MgEHO with hexylamine and octanal. Magnesium(II) porphyrins have the tendency to axially bind a fifth and sixth ligand sequentially. It is clear in the literature that hard ligands (such as oxygen and nitrogen) are greatly favored over soft and that the binding of nitrogenous bases is stronger than that of oxygen containing ligands.[19]

Sn(IV) porphyrins are known to bind strongly to oxygen containing ligands such as alcohols to form 6-coordinate complexes.[20] Although in our experiments no response is observed for SnEHO exposed to any of the analytes, there may still be some interaction occurring with the alcohol. The SnEHO when synthesized already has two axial hydroxy ligands to satisfy the +4 oxidation state of the Sn metal atom; exchanging these hydroxy ligands for other groups may not affect the absorption spectrum significantly, and hence, no appreciable optical response would be observed.

The interaction upon exposure of 2 mL of the four EHO solutions to the different analytes is summarized in Figure 5. The difference between the unexposed and exposed spectra was calculated and then squared (such that all differences are

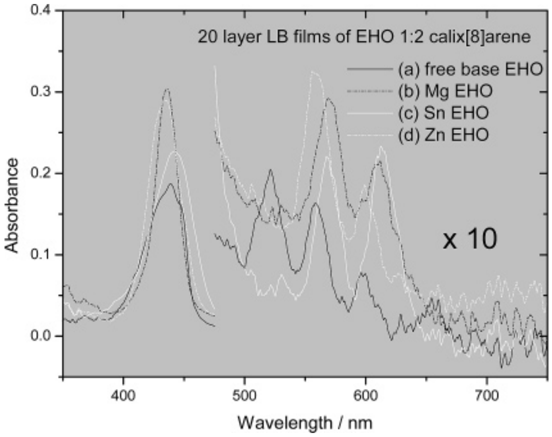

Figure 6. Absorbance spectra for (a) free base EHO/calix[8]arene (solid black), (b) Mg EHO/calix[8]arene (dashed black), (c) Sn EHO/calix[8]arene (solid white), and (d) Zn EHO/calix[8]arene (dashed white) LB films on glass substrates (the spectra from 475 to 750 nm have been multiplied by 10).

positive). The data plotted in Figure 5 is the average of the squared difference in the range 350−750 nm. It is evident that there is a strong interaction between the free base EHO with acetic acid and trimethyl phosphite. ZnEHO also reacts strongly with the amines hexylamine, octylamine, and to a lesser degree triethylamine. Therefore, these interacting sensor/analyte pairs were investigated further when transferred to solid-state LB films.

Previous work[17] has shown that upon transferring EHO from a solution to an LB film the absorption bands broaden, implying that there is a slight increase in the inhomogeneity of the local environment of the EHO molecules in the LB films compared to the solution. This is most likely due to the occurrence of J (or edge-to-edge) aggregate formation in the EHO films.[21−23] The presence of such J aggregates is thought to reduce the sensitivity of the EHO as a sensor material. To reduce any aggregate formation in the solid-state LB films used in this study the EHOs were mixed with calix[8]arene which is optically inert in the wavelength range of interest and makes high quality LB films. This process is known to improve the quality of the films formed for free base EHO, and it dramatically improves the sensor dynamics of this material as an NO_2 sensor.[17] The solid-state film of pure free base EHO does not switch completely upon exposure to NO_2, whereas in contrast for the mixed free base EHO/calixarene films little evidence of the original EHO absorption spectra features remains after NO_2 exposure, indicating a much more complete switching process for the EHO/calix[8]arene mixture. This improvement in the film quality was most marked for the free base EHO, and similar improvements in the LB film quality were found for the Mg, Sn, and Zn EHO/calix[8]arene LB films. Therefore, all four EHO materials used in this study were mixed with calix[8]arene when being transferred to solid-state films.

When the EHOs from solution were transferred to a solid-state LB film, the wavelengths of the Soret absorption feature are slightly red-shifted and bandwidths of all absorption features are slightly increased, indicating that the local environments of the EHO molecules have changed slightly, see Figure 6 in comparison with Figure 3. It is evident that the Soret absorption bands have broadened and shifted to the longer wavelengths. The Soret peaks in the solid-state films are at 438, 436, 442, and 435 nm for free base EHO, MgEHO, SnEHO, and ZnEHO, respectively. These red shifts are thought to be partly due to the effect of removing the solvent and partly due to aggregation effects upon transfer to an LB film, despite having mixed the porphyrins with calix[8]arene to minimize any aggregation effects.

The results from the solution experiments summarized in Figure 5 were used to guide the choice of sensor/analyte pairs that were chosen for further investigation as solid-state films. Sensor/analyte pairs that displayed wavelength red shifts greater than 2 nm and absorbance intensity changes greater than ±10% were selected for further investigation. Therefore, the interactions of the sensor films with the amine analytes (looking at ZnEHO in particular), trimethyl phosphite (looking at free base EHO in particular), and acetic acid were studied.

Figure 7a compares the spectra measured for the ZnEHO film before and after exposure to hexylamine at 48 °C, and Figure 7b shows the absorbance at 435 nm (the Soret absorption peak for ZnEHO/calix[8]arene films) for a ZnEHO/calix[8]arene LB film as a function of time upon exposure to hexylamine. The N_2 flow is switched between direct supplying 500 sccm clean N_2 gas or 500 sccm N_2 which has passed through the analyte chamber (maintained at 0 °C) and therefore contains analyte vapors. Exposure to the analyte for 300 s at 48 °C was followed by 300 s recovery period also at 48 °C. The concentration of hexylamine vapor during the exposure cycle is estimated by considering the vapor pressure of hexylamine at 0 °C (all analyte

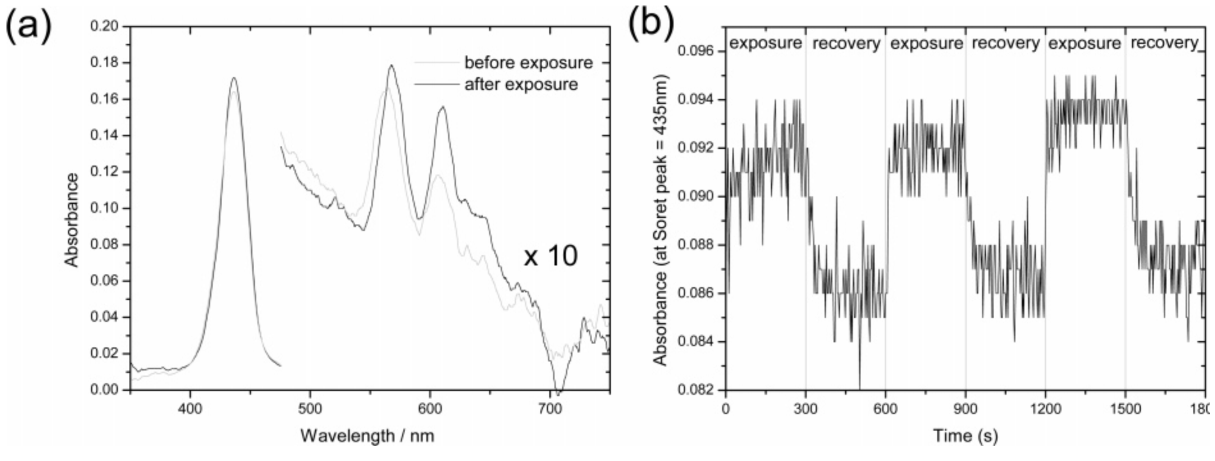

Figure 7. (a) Absorption spectra for a ZnEHO/calix[8]arene LB film before (gray) and after (black) exposure to hexylamine (estimated concentration ∼2000 ppm, the spectra from 475 to 750 nm have been multiplied by 10) and (b) the absorbance change at the ZnEHO Soret wavelength of 435 nm during three exposure (∼2000 ppm hexylamine for 300 s) and recovery (N_2 for 300 s) cycles at 48 °C for the solid-state ZnEHO/calix[8]arene film.

concentrations were estimated using data found in ref 24; no data was available for octylamine so an extrapolation between the values for pentylamine and nonylamine was used), the estimated concentration for hexylamine at 0 °C is ∼2000 ppm.

The rise time for the absorption change observed at 435 nm for a ZnEHO/calix[8]arene LB film upon exposure to hexylamine as shown in Figure 7 is very fast. The time taken to reach 50% of the complete change is ∼7 s, and the time taken to reach 90% of complete change is ∼11 s. These values are comparable for the 50% response rates for free base EHO upon exposure to NO_2 reported in ref 17, and considerably faster than the 90% response rate. The ZnEHO/calix[8]arene sensor is seen to recover when the hexylamine vapor flow is stopped. The recovery takes ∼150 s at 48 °C. It is very promising to note that after recovery the absorbance returns to approximately the same value for every cycle indicating that this system is readily reset for reuse as a sensor. It should be noted that when ZnEHO is in solution exposure to hexylamine causes a shift in the Soret absorption wavelength from 427 to 433 nm and an increase in the absorption peak. In contrast, the ZnEHO/calix[8]arene LB film experiments showed no shift in the Soret peak position; however, there is still an increase in absorbance intensity at the LB film Soret wavelength of 438 nm. Upon transfer of the ZnEHO from solution to an LB film, the Soret absorption peak is shifted from 427 to 438 nm.

As can be seen in Figure 4, the exposed solution absorption at 433 nm is stronger by ∼24% compared to the unexposed solution at 427 nm. This compares reasonably with the solid-state film which undergoes ∼8% increase (at 438 nm without any wavelength shift) upon exposure to hexylamine at 48 °C, the difference in intensity of the increase presumably being due to the larger quantity of analyte used in the solution exposure compared to the solid-state exposure and the fact that the absorbance peaks are somewhat broadened in the solid-state films. Temperature dependence of the response magnitude, as discussed later, also implies that the accessibility of the active sites of the ZnEHO molecules in the LB films plays an important role in determining the magnitude of the sensor response. The solid film response is also similar to the solution response in that the Q-band absorption peaks are slightly red shifted upon exposure and the intensity of the longer wavelength band of the two Q-bands increases significantly and a third band at even longer wavelength appears upon exposure.

In Figure 7b, the first exposure/recovery cycle has not been shown because during this cycle the absorbance level undergoes an initial increase, which is thought to be due to both stabilizing of the temperature and the removal of contaminants, such as water or oxygen, which evaporate off the film during the first cycle. In the latter cycles, i.e., those shown in Figure 7b, the absorbance returns to the same level for each of the exposed and recovered halves of the cycle.

Similar results were obtained for the interaction of ZnEHO/calix[8]arene LB film with octylamine and triethylamine. The Soret absorbance at 438 nm increased by ∼7% for the octylamine, and it increased by ∼10% for the triethylamine compared to ∼8% for hexylamine as shown in Figure 8. The different response intensities observed for the different amines are due to differences in the vapor pressure of the different amines at 0 °C (resulting in different concentrations of each amine), diffusion rates for the amines into the sensor film, and the accessibility of the nitrogen atom in the amine to form ligands with the ZnEHO. The concentrations for triethylamine, hexylamine, and octylamine estimated from their vapor pressure data are ∼14000, ∼2000, and ∼200 ppm, respectively. The influence of these parameters on the ZnEHO sensor response to amines is subject to further investigations

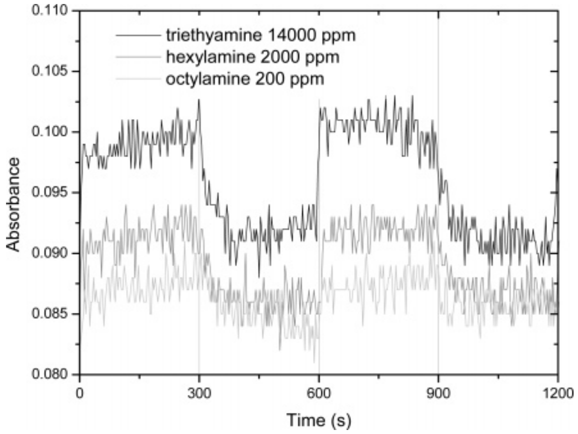

Figure 8. Comparison of the absorbance change at 435 nm during three exposure (analyte for 300 s) and recovery (N_2 for 300 s) cycles for the solid-state ZnEHO/calix[8]arene film upon exposure to the triethylamine (black), hexylamine (gray), and octylamine (light gray) at 48 °C.

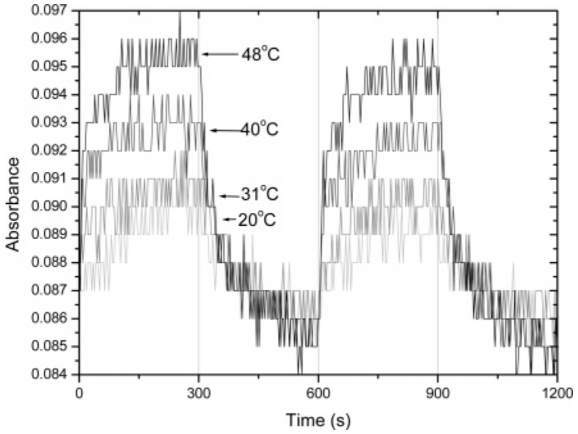

Figure 9. ZnEHO/calix[8]arene LB film response to hexylamine (∼2000 ppm) at 48 (black), 40 (dark gray), 31 (gray), and 20 (light gray) °C.

As was expected from the solution results, there were no significant absorption changes when the free base EHO/calix[8]arene LB film or the SnEHO/calix[8]arene LB film was exposed to any of the amine analytes. There was some evidence of a very weak response for MgEHO/calix[8]arene LB film exposed to hexylamine; however, it was comparable to the noise levels in measurement. The responses measured for these films displayed changes of less than 3% of the Soret intensity, which are within the margins of experimental error.

As the temperature of the ZnEHO/calix[8]arene LB film was increased from 20 up to 48 °C, the response to amine was found to increase. Figure 9 shows the variation of the ZnEHO/calix[8]arene LB sensor response as a function of temperature upon exposure to hexylamine (estimated concentration ∼2000 ppm). Similar trends were observed for the ZnEHO upon exposure to octylamine and triethylamine. It is thought that the increasing temperature improves the sensor response by improving the accessibility of the active site of the ZnEHO, either by improving the diffusion of the analyte species through the film or by removing other gaseous species that may occupy the sites without causing a spectral change.

There was no significant response measured for any of the four EHO/calix[8]arene LB films upon exposure to either acetic acid or trimethyl phosphite. In all cases, the exposure to acetic acid or trimethyl phosphite resulted in changes of less than 3% of the Soret intensity (the estimated experimental margin of error). This was surprising since the solution experiments showed a very strong response for acetic acid interacting with the free base EHO and a weaker interaction for the acetic acid and MgEHO. It would appear that the reaction can only occur when the acid can freely dissociate in solution, whereas in gaseous form the acetic acid cannot dissociate and therefore cannot protonate the free base EHO. Similarly, the strong interaction between trimethyl phosphite and free base EHO only occurs in the solution experiments; the exact nature of this interaction is uncertain.

Conclusions

In solution, there are strong responses upon exposure for ZnEHO and all three amines investigated. Both trimethyl phosphite and acetic acid produced strong interactions with the free base EHO, and MgEHO and acetic acid produced a weak interaction which is thought to be due to the conversion of the MgEHO back into free base EHO by action of the acid followed buy a free base EHO interaction with acetic acid.

When transferred to solid-state LB films, aided by mixing with calix[8]arene, only some of the interactions observed in the solution experiments continue to occur. There is no optical change observed upon exposure of the free base EHO/calix[8]-arene LB films to vapors of either acetic acid or trimethyl phosphite, and similarly there is no response when MgEHO/calix[8]arene LB films are exposed to acetic acid. The ZnEHO/calix[8]arene LB films, however, do continue to respond to the three amines investigated. Therefore, ZnEHO/calix[8]arene LB films have been demonstrated to be effective solid-state amine sensors. The response for the ZnEHO/calix[8]arene LB films to amines increases with increasing temperature in the range 20−48 °C and also depends on the analyte concentration and the amine structure.

Acknowledgment. Financial support of this work by the EPSRC (UK) Grant GR/596845/01 is gratefully acknowledged, as is the advice of Dr. W. Barford.

References and Notes

(1) http://europa.eu.int/comm/environment/air_en.htm, May 2006.

(2) http://www.environment-agency.gov.uk/subjects/airquality/?lang=_e, May 2006.

(3) Mandelis; Christofides, C. *Physics, Chemistry, and Technology of Solid State Gas Sensor Devices*; Wiley-Interscience Publications: New York, 1993.

(4) Albert, K. J.; Lewis, N. S.; Schauer, C. L.; Sotzing, G. A.; Stitzel, S. E.; Vaid, T. P.; Walt, D. R. *Chem. Rev.* **2000**, *100*, 2595.

(5) Moseley, P. T.; Norris, J. O. W.; Williams, D. E. *Techniques and Mechanisms in Gas Sensing*; Adam Hilger: Bristol, U.K., 1991.

(6) Lonergan, M. C.; Severin, E. J.; Doleman, B. J.; Beaber, S. A.; Grubb, R. H.; Lewis, N. S. *Chem. Mater.* **1996**, *8* (9), 2298.

(7) Capone, S.; Mongelli, S.; Rella, R.; Siciliano, P.; Valli, L. *Langmuir* **1999**, *15*, 5 (5), 1748.

(8) George, C. D.; Richardson, T.; Hofton, M. E.; Vale, C. M.; Neves, M. G. M.; Cavaleiro, J. A. S. *Mater. Sci. Eng., C* **1999**, *8−9*, 559.

(9) Richardson, T.; Smith, V. C.; Johnstone, R. A. W.; Sobral A. J. F. N.; Rocha-Gonsalves, A. M. d'A. *Thin Solid Films* **1998**, *327−329*, 3151.

(10) Dooling, C. M.; Worsfold, O.; Richardson, T. H.; Tregonning, R.; Vysotsky, M. O.; Hunter, C. A.; Kato, K.; Shinbo K.; Kaneko, F. *J. Mater. Chem.* **2001**, *11*, 392.

(11) Worsfold, O.; Dooling, C. M.; Richardson, T. H.; Vysotsky, M. O.; Tregonning, R.; Hunter, C. A.; Malins, C. *J. Mater. Chem.* **2001**, *11*, 399.

(12) Pedrosa, J. M.; Dooling, C. M.; Richardson, T. H.; Hyde, R. K.; Hunter, C. A.; Martín, M. T.; Camacho, L. *J. Mater. Chem.* **2002**, *12*, 2659.

(13) Suslick, K. S.; Rakow, N. A.; Sen, A. *Tetrahedron* **2004**, *60*, 11133.

(14) Sanders, J. K. M.; Bampos, N.; Clyde-Watson, Z.; Darling, S. L.; Hawley, J. C.; Kim, H.-J.; Mak, C. C.; Webb, S. J. The axial coordination chemistry of metalloporphyrins. *The Porphyrin Handbook*; Academic Press: New York, 1999; Vol. 3, Chapter 15.

(15) Gutsche, C. D. *Calixarenes, Monographs in Supramolecular Chemistry*; Royal Society of Chemistry: London, 1989.

(16) Taylor, P. N.; Anderson, H. L. *J. Am. Chem. Soc.* **1999**, *121*, 11538−11545.

(17) Dunbar, A.; Richardson, T. H.; McNaughton, A. J.; Barford, W.; Hutchinson, J.; Hunter, C. A. *Colloids Surf., A* **2006**, *284−285*, 339−344.

(18) Dolphin, D. *The Porphyrins: Structure and Synthesis, Part A, Vol. 1*; Academic Press: London, 1978.

(19) Kadish, K. M.; Shuie, L. R. *Inorg. Chem.* **1982**, *21*, 1112.

(20) Holloway, C. E.; Melnik, M. *Main Group Met. Chem.* **1998**, *21*, 371.

(21) Pedrosa, J. M.; Dooling, C. M.; Richardson, T. H.; Hyde, R. K.; Hunter, C. A.; Martín, M. T.; Camacho, L. *Mater. Sci. Eng.* **2002**, *C22*, 433.

(22) Chou, H.; Chen, C.-T.; Stork, K. F.; Bohn, P. W.; Suslick, K. *J. Phys. Chem.* **1994**, *98*, 383.

(23) Kroon, J. M.; Sudhölter, E. J. R. *Langmuir* **1995**, *11*, 214.

(24) *CRC Handbook of Chemistry and Physics*; Lide, D. R., Ed.; CRC Press: Boca Raton, FL, 2005.